EQUIVALENT MODELLING AND SUPPRESSION OF AIR RESONANCE FOR THE ACT/FHS IN FLIGHT

Steffen Greiser and Robin Lantzsch
Steffen.Greiser@dlr.de, Robin.Lantzsch@dlr.de
German Aerospace Center (DLR), Institute of Flight Systems
Lilienthalplatz 7, 38108 Braunschweig, Germany

ABSTRACT

Closed-loop controllers assist helicopter pilots in flight and improve handling qualities compared to bare-airframe control. For high feedback gains (especially roll rate to lateral control input), mainly a roll oscillation can be observed which is often called air resonance. In previous work, the air resonance was successfully modelled and suppressed for the ACT/FHS. Today, new research tasks were defined that require full-state feedback and excellent model-based control performance. The new tasks require better controller performance and with this an adaptation of the air resonance suppression. Additionally, the ACT/FHS has now an engine upgrade, new lead-lag dampers and a higher landing skid and a sensor suite for enhanced vision. The new configuration may cause changes of air resonance dynamics. This paper will focus on three major topics, that are flight test procedure, modelling and air resonance suppression. The data as well as the respective model changes are compared to the previous results. The adapted air resonance suppression presented in this paper has slightly better performance than the previous one. This is a promising intermediate result for the usage of the model-based control in future work.

NOTATION

a_x, a_y, a_z	linear accelerations
$\mathbf{A}_{11}, \mathbf{A}_{12},$ $\mathbf{A}_{21}, \mathbf{A}_{22}$	partitions of the system matrix **A**
A, **B**, **C**, **D**	linear state-space matrices
ARS	air resonance suppression
b_1, b_2	numerator's coefficients
$\mathbf{B}_1, \mathbf{B}_2$	partitions of the input matrix **B**
$\mathbf{C}_1, \mathbf{C}_2$	partitions of the output matrix **C**
D	damping coefficient
D	feedthrough matrix
$G_{11}, G_{12},$ G_{21}, G_{22}	SISO-systems representing regressive lead-lag
G_{ll}	lead-lag SISO representation
G_{py}	SISO roll representation
$\mathbf{G}_{\mathbf{x}_1}$	frequency representation of the helicopter model without regressive lead-lag
$\mathbf{G}_{\Delta}$	lead-lag frequency representation
I	unity matrix
K_p	roll rate feedback gain
K_y	gain for lateral cyclic control for air resonance suppression
L, M, N	aerodynamic moments
p, q, r	angular velocities
s	Laplace variable
u, v, w	body-axis velocities
$\mathbf{u}, \mathbf{U}(s)$	control vector: time & frequency domain
$\mathbf{u}_z, \mathbf{U}_z(s)$	control vector with disturbance
w_h	non-physical state
x	state vector
X, Y, Z	aerodynamic forces
$x_{ll,1}$ $x_{ll,2}$	lead-lag states due to δ_x
$\mathbf{x}_1$	remaining states, without lead-lag
$\mathbf{x}_2$	lead-lag states
X_1, X_2	lead-lag parameters (longitudinal)
y	output vector
$y_{ll,1}$ $y_{ll,2}$	lead-lag states due to δ_y
Y_1, Y_2	lead-lag parameters (lateral)
$\mathbf{Y}(s)$	transformed output vector
z	disturbances
$\mathbf{Z}(s)$	transformed disturbances
$\delta_x, \delta_y, \delta_p, \delta_0$	longitudinal, lateral, pedal, collective control inputs
$\Delta\mathbf{x}_1$	additional state vector, for lead-lag
δ_y	lateral control to the actuator
$\delta_{y,EP}$	reference value
Δ_y	lateral control to the actuator given in frequency domain
$\Delta_{y,z}$	lateral control and input for δ-ARS
$\mathbf{\Lambda}$	scaling matrix
ϕ, θ	roll and pitch angles
ω_0	eigenfrequency

1. INTRODUCTION

Feedback controllers are widely used to stabilize the rotorcraft and to ease flying. Rate feedback is commonly used to increase damping and bandwidth resulting in better handling qualities. However, rate feedback can lead to lightly damped roll oscillations, which may become unstable with increasing feedback gain. Soft-in-plane rotors (rotors with a regressive lead-lag frequency that is lower than the shaft rotational speed) such as hinge- or bearingless main rotors for instance suffer from this phenomenom termed as air resonance. For example, in the case of DLR's ACT/FHS, air resonance is mainly noticed by the pilot as an oscillatory ringing in the helicopter roll response. More specifically, the air resonance mode may become unstable when roll rates are fed back on lateral cyclic control. Without rate feedback the lightly damped oscillation is below the pilot's perception level and cannot be separated from the regular EC135 dynamics. Since most of the flight control concepts used today need roll rate feedback, this is an undesired and disagreeable effect which has to be suppressed. The phenomenon is well described in [1]. Transforming the lead-lag blade motion to the non-rotating frame it looks like that the centre for gravity whirl around the centre of the rotor disk. This effect may excite body natural modes. The lead-lag motion is composed of three dynamic systems (that are typically described as second order systems) which are regressive lead-lag, advancing lead-lag and collective lag mode. Especially regressive lead-lag with its lower-frequency oscillation mainly affects the roll motion. The frequency can be calculated by subtracting the blade lead-lag frequency from the rotor frequency. However, if the pilot feels this disturbing oscillation of the fuselage, handling qualities may become worse.

In the past decade, numerous efforts have been made worldwide to model and to simulate the air resonance mode and to develop active controller schemes in order to suppress the oscillation. In [2] the mechanisms, through which the pilot or the flight control system (FCS) excite the air resonance when using roll rate feedback, are studied. In [3, 4] the feedback of body roll and pitch angles, rates and accelerations is proposed to increase stability. In [5], additionally, the effect of multiblade cyclic lead-lag angle, rate and acceleration feedback on aeromechanical stability is studied. The study demonstrates that blade lead-lag states can be used for feedback instead of body states and vice versa. [6] shows, that if properly filtered, the roll rate can be used as feedback instead of roll acceleration, if there is no roll acceleration signal available. In [7, 8] an approach is suggested in which Individual Blade Control (IBC) is used to increase lead-lag damping and aeromechanical stability. This is done by feedback of the lead-lag rate. In [9, 10] a cross feed approach is described, in which roll rate is filtered and fed back on the longitudinal axis and filtered pitch rate is fed back on the lateral axis. In the development of the military helicopter RAH-66 Comanche, good results were obtained using this approach. With [11, 12] DLR demonstrates the first approach using a dipole cancelling control. That controller calculates an adapted roll rate which is used for feedback. This works well but yield inconsistent measurements which is disturbing if full-state feedback is used.

The dipole cancelling controller is used to improve handling qualities and is one component of the model-based control [13]. This controller is used for assistance systems [13] and is flight-tested using the research helicopter ACT/FHS (Active Control Technology/Flying Helicopter Simulator) shown in figure 1. The ACT/FHS testbed is based on a Eurocopter EC135, a light, twin-engine helicopter with bearingless main rotor and fenestron. Its mechanical controls are replaced by a full-authority fly-by-wire/fly-by-light primary control system, which allows changes of the control inputs applied to the helicopter by an experimental system [14]. Because of the replaced mechanical controls the dynamic data shown in this paper are not comparable to data from series-production rotorcraft. In combination with a wide range of different sensors the ACT/FHS is used in multiple research projects in the fields of flight control, pilot assistance and handling qualities.

Figure 1: DLR's research helicopter ACT/FHS

The major goal of this paper is to derive a suppression method that does not alter roll rate. New research tasks concern rotor-state feedback and require the feedback of higher order derivatives. It is desired to have consistent measurements used for helicopter control. Thus the dipole cancelling controller is redesigned for full-state feedback. The design and structure of the full-state feedback is kept comparable to rotorcraft that do not have air resonance at lower frequencies. One opportunity, presented in this paper, is to suppress air resonance with an additional control signal. Two air resonance suppression (ARS) methods are compared to one another, that are

- p-ARS: suppression of air resonance using a transformed or adapted roll rate for feedback [11, 12]
- δ-ARS: suppression of air resonance with additional control signals

This paper describes system identification for the bare-airframe helicopter in chapter 3. For a dedicated design of the air resonance suppression, the bare-airframe models are tuned based on results obtained with partial closed-loop control, chapter 4. With this, an appropriate model is obtained which is also used for the nonlinear helicopter simulation, chapter 5. Finally, three models are obtained that are:

- original model: bare-airframe identification without any controllers active [15]
- tuned model: linear models (i.e. original models) that have adapted parameters so that the air resonance oscillation can be predicted [11]
- equivalent model: extracted, equivalent model (extracted from the tuned model) that simulate the oscillation and is used for the nonlinear helicopter simulation (ground-based simulator)

The models are used to derive the air resonance suppression (i.e. δ-ARS). With the nonlinear helicopter simulation, a feasible flight test approach for the ACT/FHS was derived and is presented in chapter 6. The respective flight test results are shown in chapter 7.

2. Overview and Problem

As a typical example figure 2 demonstrates the effect of the air resonance mode on the performance of the ACT/FHS ACAH type of controller. The blue dashed lines represent the required response and the green solid lines the measured response. Mainly, a persistent roll oscillation at the air resonance frequency of about 11.5 $^{rad}/_{s}$ can be observed. It can also be seen that, even with a perceptible oscillation in roll rate, the roll angle does only show minor oscillations. The coupling of the roll oscillation on pitch is nearly non-existent.

The respective ACT/FHS ACAH type of controller was designed based on a linear state-space model derived by system identification [15]. The oscillation was not expected by the controller design though an identified model is used. However, in flight tests with the EC135 ACT/FHS the designed controllers become unstable for high feedback gains. Mainly, the roll axis response was oscillating due to high feedback gains. The goal is to reduce the oscillation observed in flight by keeping the high feedback gains and with this to realise fast roll response. This, however, requires an algorithm to suppress the oscillation. And to further allow a model-based design rather than an empirical one, the linear model derived by system identification has to be improved.

In general, system identification is applied to data of the EC135 ACT/FHS that are obtained without any controller assistance. With this, linear models for the regressive lead-lag at distinct operating points (depending on airspeed) are identified. First of all an overview about the open-loop test techniques will be given.

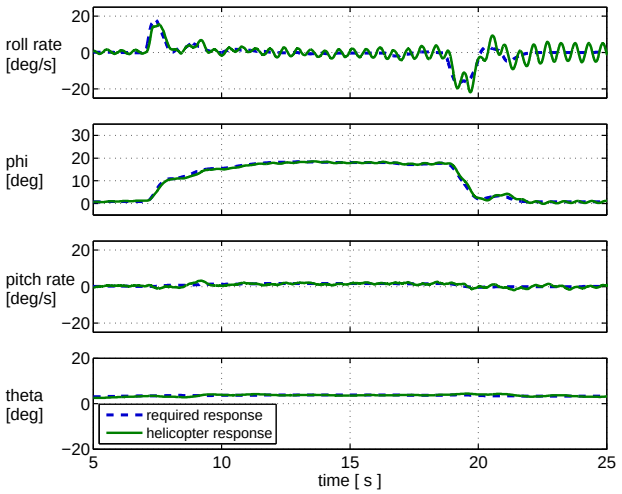

Figure 2: Model-based control without air resonance suppression

3. System Identification With Open-Loop Test Techniques

System identification is performed for the bare airframe helicopter without feedback controllers. Frequency sweep data are used for the identification in frequency domain [16]. With this, linear models are derived and the model complexity depends on the frequency range of interest (approx. 1-20 $^{rad}/_{s}$). From experience and model validation data, the minimum order of the identified state-space model is determined empirically based on physics-based modelling [15]. The ACT/FHS models are used for controller development and account for rigid body dynamics, first-order rotor flapping, regressive lead-lag and mean inflow. Rotor flapping can be described by the longitudinal and lateral deflection of the main rotor's tip-path plane [17] and the respective model is explicitly formulated. For the EC135 ACT/FHS models, the explicit formulation is replaced by an implicit one that uses roll and pitch acceleration instead of the tip-path plane's deflection. The lead-lag motion is modelled with second-order systems using lateral and longitudinal controls as inputs. The mean inflow primarily has an influence on the vertical translatory motion due to collective control. An implicit formulation together with a minimal realization is used that leads to the non-physical state w_h [18]. Finally, a 15th-order state-space model is obtained that shows adequate matching results.

The measurements (i.e. frequency sweep data) show a slightly low-damped oscillation at approx. 11.5 $^{rad}/_{s}$. For lateral control, the regressive lead-lag influences mainly roll

p but also pitch q, yaw r and vertical velocity w. If those measurements and especially roll rate would be used for feedback control, the closed-loop may become unstable for high feedback gains as depicted in figure 2. The body-fixed velocities u, v are not analysed explicitly in this paper as the respective control-loop (velocity hold) has small gains and imposes a slow dynamic so that regressive lead-lag has little effect on stability margins. Figure 3 shows the computed frequency response for lateral control at 60 knot forward flight. The angular rates are strongly affected by regressive lead-lag and vertical velocity is characterised by only small amplitudes.

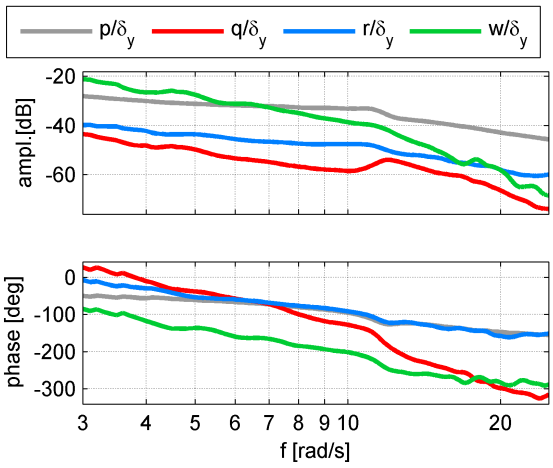

Figure 3: Computed frequency response data for lateral control δ_y[%] to the states p [rad/s], q [rad/s], r [rad/s] and w [m/s] at 60 knot forward flight

The corresponding longitudinal control is shown in figure 4. Again, the computed frequency response at 60 knot forward flight is depicted and the angular rates are strongly affected by regressive lead-lag. The effect of regressive lead-lag cannot be observed for the vertical velocity.

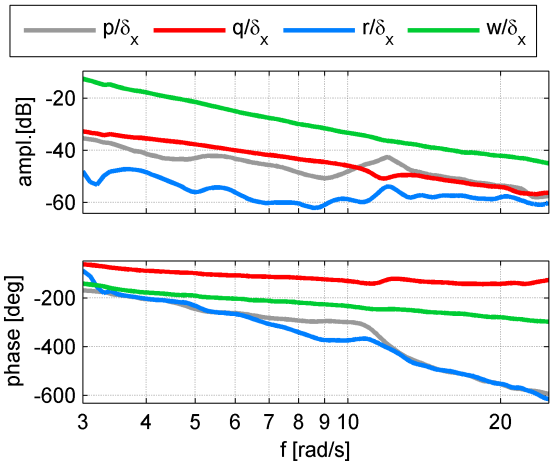

Figure 4: Computed frequency response data for longitudinal control δ_x[%] to the states p [rad/s], q [rad/s], r [rad/s] and w [m/s] at 60 knot forward flight

Similar plots can also be generated for pedal and collective control. Pedal control does not excite the regressive lead-lag. Collective excites the lead-lag oscillation and its effect can be observed for the angular rates but not for the vertical velocity. This can also be repeated for all velocities, i.e. for system identification purposes hover, 30 knot, 60 knot, 90 knot, 120 knot. For 60 knot, table 1 shows whether the lead-lag oscillation could be observed or not. This analysis is data driven and is performed empirically and may help to define an appropriate model structure for system identification purposes.

	pitch rate	roll rate	yaw rate	vertical velocity
longitudinal	$\surd$	$\surd$	$\surd$	$\emptyset$
lateral	$\surd$	$\surd$	$\surd$	$\surd$
pedal	$\emptyset$	$\emptyset$	$\emptyset$	$\emptyset$
collective	$\surd$	$\surd$	$\surd$	$\emptyset$

Table 1: Observed regressive lead-lag oscillation for bare-airframe using frequency sweeps, $\emptyset$ - not observed, $\surd$ - observed

The linear system is described as follows

$$\begin{aligned}\dot{\mathbf{x}} &= \mathbf{A}\mathbf{x} + \mathbf{B}\mathbf{u} \\ \mathbf{y} &= \mathbf{C}\mathbf{x} + \mathbf{D}\mathbf{u}\end{aligned} \tag{1}$$

$$\mathbf{A} \in \mathbb{R}^{n\times n},\ \mathbf{B} \in \mathbb{R}^{n\times m},\ \mathbf{C} \in \mathbb{R}^{l\times n},\ \mathbf{D} \in \mathbb{R}^{l\times m}$$

The state vector $\mathbf{x}$ consists of the remaining states $\mathbf{x}_1$ and the lead-lag states

$$\mathbf{x} = [\mathbf{x}_1\ x_{ll,1}\ x_{ll,2}\ y_{ll,1}\ y_{ll,2}]^T = [\mathbf{x}_1\ \mathbf{x}_2]^T \tag{2}$$

$$\mathbf{x} \in \mathbb{R}^n,\ \mathbf{x}_1 \in \mathbb{R}^{\tilde{n}}$$

where the remaining states $\mathbf{x}_1$ are

$$\mathbf{x}_1 = [u, v, w, p, q, r, w_h, \dot{p}, \dot{q}, \phi, \theta]^T \tag{3}$$

The controls are longitudinal, lateral, pedal and collective control so that:

$$\mathbf{u} = [\delta_x, \delta_y, \delta_p, \delta_0]^T \tag{4}$$

The outputs $\mathbf{y}$ are similar to the states except that the linear accelerations a_x, a_y, a_z as well as yaw acceleration are taken into account and that the nonphysical state w_h as well as lead-lag states are not considered.

$$\mathbf{y} = [u, v, w, p, q, r, \dot{p}, \dot{q}, \dot{r}, \phi, \theta, a_x, a_y, a_z]^T \tag{5}$$

Lead-lag dynamics are driven by the longitudinal and lateral control and have mainly a contribution to the roll and pitch response. The extracted equations from the state-space

model considering lead-lag are (green - longitudinal, blue - lateral):

$$
\begin{aligned}
\ddot{p} =& L_u u + \cdots + L_{x_{ll,1}} x_{ll,1} + L_{x_{ll,2}} x_{ll,2} + \\
& L_{y_{ll,1}} y_{ll,1} + L_{y_{ll,2}} y_{ll,2} + L_{\delta_x} \delta_x + L_{\delta_y} \delta_y \\
\ddot{q} =& M_u u + \cdots + M_{x_{ll,1}} x_{ll,1} + M_{x_{ll,2}} x_{ll,2} + \\
& M_{y_{ll,1}} y_{ll,1} + M_{y_{ll,2}} y_{ll,2} + L_{\delta_x} \delta_x + L_{\delta_y} \delta_y \\
\dot{x}_{ll,1} =& x_{ll,2} \\
\dot{x}_{ll,2} =& X_1 x_{ll,1} + X_2 x_{ll,2} + \delta_x \\
\dot{y}_{ll,1} =& y_{ll,2} \\
\dot{y}_{ll,2} =& Y_1 y_{ll,1} + Y_2 y_{ll,2} + \delta_y
\end{aligned}
\tag{6}
$$

The parameters of the state-space system such as $L_u, M_u, L_{x_{ll,1}}, \cdots$ are estimated with frequency methods [16]. The parameters X_1, X_2, Y_1, Y_2 are the derivatives of the pole of the regressive lead-lag. The models derived by system identification have an acceptable match with the measurements [18, 19]. As one example, the roll rate due to lateral control at 60 knot is depicted in figure 5. Especially, the roll rate has an excellent match. Although, a good match can be observed, the oscillation as introduced with figure 2 cannot be predicted. The reason for this is not analysed in this paper but may be an effect of a nonlinear damping characteristic. The goal is just to have a model of the plant that predicts this type of oscillation for high feedback gains.

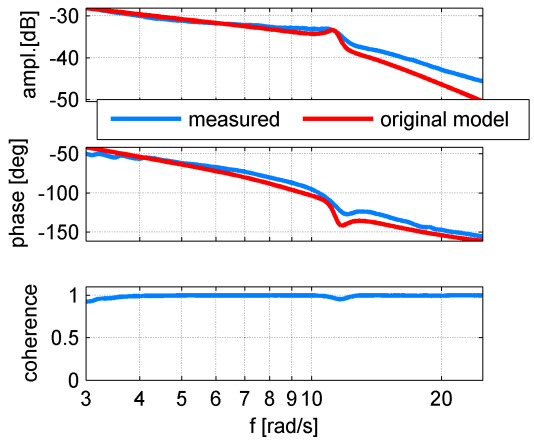

Figure 5: Comparison between system identification result (red) and computed frequency response (blue, based on time-domain measurements) at 60 knot forward flight for roll rate p [rad/s] due to lateral control δ_y[%]

To give the reader more insight, an approximation of the low-order system for roll rate due to lateral control is (using SI-units)

$$
\begin{aligned}
\frac{p}{\delta_y} &= \frac{1.716}{s^2 + 10s + 60} \cdot G_{ll} = G_{py} \\
G_{ll} &= \frac{s^2 + 2.4s + 135}{s^2 + 1.6s + 130}
\end{aligned}
\tag{7}
$$

Here, G_{ll} denotes the second order system for regressive lead-lag modelling. The system G_{py} approximates the system identification results (red curve) as depicted in figure 5.

As previously stated, the identified models do not predict air resonance for the closed-loop control. Air resonance is mainly excited if roll rate is fed back on lateral cyclic control. This control loop without any other controllers active is called partially closed-loop control. As one example respective flight test data of this control-loop for $K_p = 60$ are shown in figure 6. The grey curves are the measurements and the red curves are the simulation results obtained with the identified model at 60 knot (original model). The frequency of the air resonance is at approximately f = 1.8 Hz and the alternating step of the lateral control has a duration of Δt = 1/1.8 s to excite the oscillation. The stick inputs corresponds to the reference values and are not the actuator signals. With a high feedback gain, an oscillating roll rate is measured. This oscillation cannot be predicted using the linear models derived by system identification (red curve in figure 6).

Using the approximated roll dynamic (equation (7)) together with the feedback controller $G_C = 60$, the closed-loop is

$$
\begin{aligned}
\frac{p}{\delta_{y,EP}} &= \frac{G_{py}}{1 + G_{py} \cdot G_C} \\
&= \frac{1.75(s^2 + 2.4s + 135)}{(s^2 + 10.2s + 157) \cdot (s^2 + 1.4s + 140)}
\end{aligned}
\tag{8}
$$

$\delta_{y,EP}$ denotes reference value whereat δ_y is the control input for the actuator. The reference values are defined by the stick inputs of the experimental pilot, [14]. With this example, the roll rate response of the original model (red curve in figure 6) can be simulated and is just given to provide more insight into compensation and suppression of air resonance.

The main purpose of the linear models derived by system identification should be to provide an offline or desktop simulation for controller development. The bare-airframe models are not sufficient to predict the closed-loop behaviour and require an improvement to predict the oscillations. To further increase accuracy, the models are tuned in the same way as proposed in [11, 12].

4. Regressive Lead-Lag Identification Using Partially Closed-Loop Control

One opportunity to improve the prediction of air resonance is to tune certain model parameters of the bare-airframe model (i.e. original model, equations (1-6)). The goal is to obtain a model that simulates the resonance phenomenon if feedback controllers are used. A self-evident technique is to use feedback controllers to excite the air resonance and to use the respective data for parameter estimation.

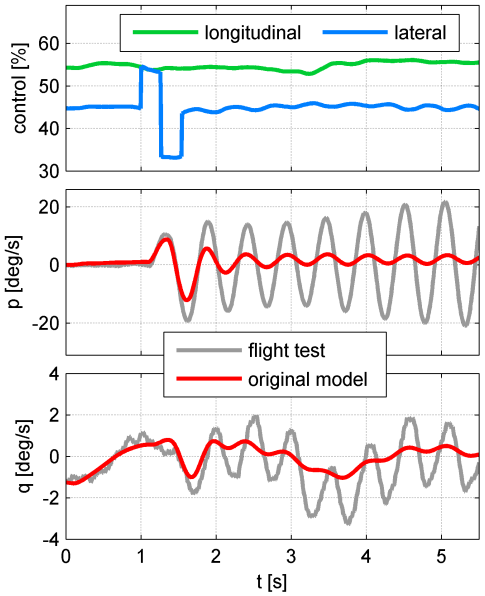

Figure 6: Roll and pitch rate response due to lateral control at 60 knot forward flight of the EC135 ACT/FHS, feedback gain $K_p = 60$, the original model is based on frequency sweep data of the bare-airframe helicopter

A simple roll rate feedback is sufficient to excite this oscillation. A schematic overview is given in figure 7.

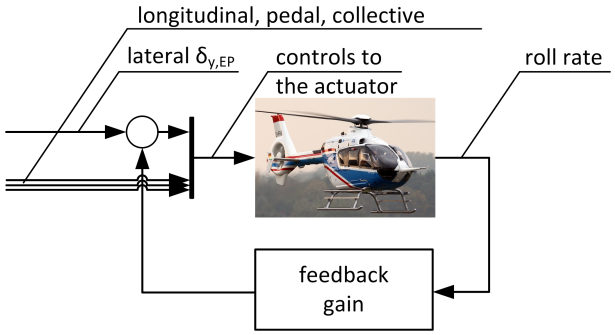

Figure 7: Partially closed-loop controller consisting of a roll rate feedback

For identification purposes, the feedback gain was $K_p = [10, 20, \cdots, 60]$. For each setting, three runs were conducted to reduce uncertainties so that finally 18 runs are available for identification.

The subset of parameters due to lateral control is analysed, i.e. $L_{y_{ll,1}}, L_{y_{ll,2}}, Y_1$ and Y_2, equation (6). The pole for regressive lead-lag is fixed, i.e. $X_1 = Y_1$, $X_2 = Y_2$. The remaining parameters are insensitive to the oscillation observed in flight. The state equation is taken from system identification results equation (1).

$$\begin{aligned} \dot{\mathbf{x}} &= \mathbf{A}\mathbf{x} + \mathbf{B}\mathbf{u} \\ p &= [0, 0, 0, 1, 0, \cdots, 0]\,\mathbf{x} \end{aligned} \tag{9}$$

The parameter estimation is performed in time domain and the error between simulated and measured roll rate (p_i and $p_{meas,i}$, respectively) is minimised for all runs $i = 1, \cdots, 18$. The parameters $\boldsymbol{\Theta}$ are estimated such that the best match for all flight test data is obtained.

$$\begin{aligned} &\min_{\boldsymbol{\Theta}} \sum_{i=1}^{N=18} (p_i - p_{meas,i})^T (p_i - p_{meas,i}) \\ &\boldsymbol{\Theta} = \left[L_{y_{ll,1}}, L_{y_{ll,2}}, Y_1, Y_2\right] \\ &s.t.\ X_1 = Y_1,\ X_2 = Y_2 \end{aligned} \tag{10}$$

Compared to [12], the feedback gain needed to excite the oscillation is $K_p = 60$ instead of $K_p = 40$. Figure 8 shows the pz-map. The 2007 data (referred to as old data, black dots) were gathered with standard engine (T1) and small landing skid. Now, the EC135 ACT/FHS has an engine upgrade (T2+) and higher landing skid together with sensors for enhanced vision installed at the landing skid (2012 data, referred to as new data, red triangles). The reason for the different K_p-values needed to excite air resonance may be caused by a changed configuration of the EC135 ACT/FHS and matured lead-lag dampers but is not known for sure as there were several configuration changes. Additionally, the pole distribution obtained with the original model (green dots) clearly show that high feedback gains do not excite air resonance. The respective time-domain result for the original model with $K_p = 60$ in figure 6 (red curve) shows the same effect.

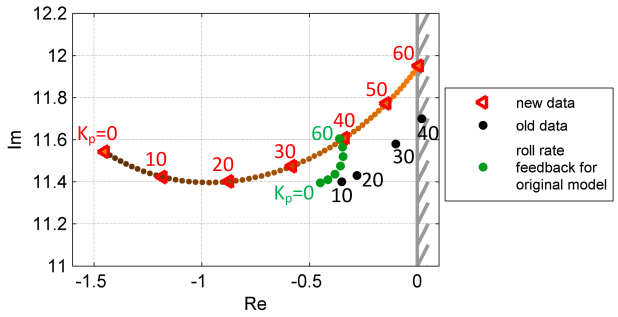

Figure 8: pn-map at 60 knot forward flight of the original model (green, [15]), new 2012 flight test data (red) and old 2007 flight test data (black, [12])

The new data (red triangles, figure 8) presented in the pz-map are a result of the parameter tuning based on equation (9). As the pz-map emphasise, the tuned model is capable to simulate the air resonance. As one example, the response due to lateral control at 60 knot is given in figure 9. The red curve designates the simulation result of the tuned model. Although the error of pitch rate was not considered by equation (9), the respective time response is predicted quite good.

The results shown in figure 9 are obtained for the multivariate state-space model, equation (1). Again, a simple SISO-system (single input single output) is given to provide more

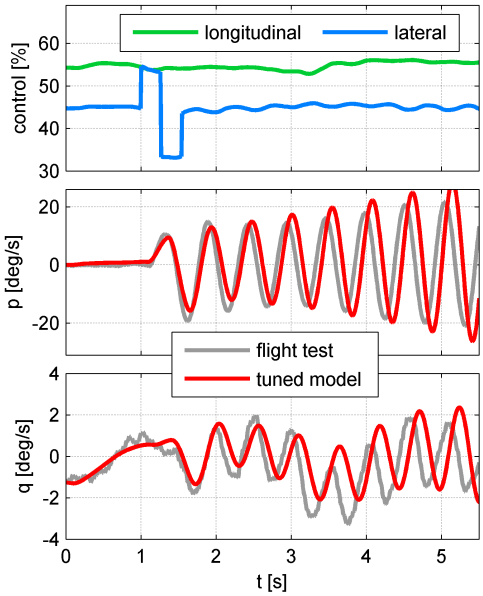

Figure 9: Roll and pitch rate response due to lateral control at 60 knot forward flight of the EC135 ACT/FHS, feedback gain $K_p = 60$, tuned model

insight. With equation (7), the basic structure is known and the parameters of the lead-lag model G_{ll} are tuned so that the simulation result matches the measured roll rate. The tuned SISO-system is:

$$\frac{p}{\delta_y} = \frac{1.716}{s^2 + 10s + 60} \cdot G_{ll} = G_{py,tuned} \qquad G_{ll} = \frac{s^2 + 3.4s + 185}{s^2 + 2.9s + 135} \tag{11}$$

Equation (11) shows the same effect for the roll rate as the multivariate model. Compared to equation (7), the pole is shifted to slightly higher frequency and has a larger damping, that is $D \approx .25$ instead of $D \approx .16$. The zero is shifted to larger frequencies (13.6 Hz instead of 11.6 Hz) and has again slightly higher damping ($D \approx .25$ instead of $D \approx .21$).

The tuned linear model is promising for controller design. Before flight testing, the algorithms are tested with a system simulator that uses the nonlinear helicopter simulation SimH [20, 21]. The next chapter shows how the system identification results are implemented to the nonlinear helicopter simulation.

5. Equivalent Model for Nonlinear Helicopter Simulation

With the tuned parameters of the multivariate, linear model, the oscillation can be predicted. The current nonlinear helicopter simulation SimH [20, 21] need much larger feedback gains to predict the same oscillation as observed in flight. Thus, the nonlinear simulation should be adapted to yield similar simulation results.

Usually, one would tune the nonlinear model equations so that the simulator has the same behaviour as the EC135 ACT/FHS. This, however, probably would need much time for implementation.

Another, opportunity is just to use the tuned system identification results for the nonlinear simulation. It should be noted that this is non-standard and that system identification is not used to replace nonlinear helicopter modelling. In frame of this work, it is a pragmatic solution to use the identification results as those are ready for implementation.

To finally obtain a model that can be used for the nonlinear simulation, the linear state-space model has to be reformulated. Equation (6) can be partitioned into lead-lag states and the remaining ones. The matrices of the linear state-space system equation (1) are then partitioned as follows. The output equation depends only on the state vector $\mathbf{x}_1$ so that

$$\mathbf{C} = \begin{bmatrix} \mathbf{C}_1 & \mathbf{C}_2 \end{bmatrix} \quad \text{with: } \mathbf{C}_2 = \mathbf{0} \tag{12}$$

The matrices of the state equation are partitioned with subject to the state vector equation (2) where the lead-lag states are $\mathbf{x}_2$. The state and input matrices become:

$$\mathbf{A} = \begin{bmatrix} \mathbf{A}_{11} & \mathbf{A}_{12} \\ \mathbf{A}_{21} & \mathbf{A}_{22} \end{bmatrix} \qquad \mathbf{B} = \begin{bmatrix} \mathbf{B}_1 + \mathbf{\Lambda} \\ \mathbf{B}_2 \end{bmatrix} \quad \text{with: } \mathbf{A}_{21} = \mathbf{0} \tag{13}$$

$\mathbf{\Lambda}$ is an additional matrix that compensates the amplitude shift that may occur comparing the system with and the system without regressive lead-lag. The state equation without lead-lag dynamics (assuming $\mathbf{A}_{12} = \mathbf{0}, \mathbf{\Lambda} = \mathbf{0}$) is

$$\dot{\mathbf{x}}_1 = \mathbf{A}_{11}\mathbf{x}_1 + \mathbf{B}_1\mathbf{u} \tag{14}$$

Taken regressive lead-lag into account, the additional states $\Delta\dot{\mathbf{x}}_1$ needed to model the respective lead-lag dynamics are

$$\begin{aligned} \dot{\mathbf{x}}_2 &= \mathbf{A}_{22}\mathbf{x}_2 + \mathbf{B}_2\mathbf{u} \\ \Delta\dot{\mathbf{x}}_1 &= \mathbf{A}_{12}\mathbf{x}_2 + \mathbf{\Lambda}\mathbf{u} \end{aligned} \tag{15}$$

and the state equation with regressive lead-lag can be reformulated

$$\dot{\mathbf{x}}_1 = \mathbf{A}_{11}\mathbf{x}_1 + \mathbf{B}_1\mathbf{u} + \mathbf{z} \quad \text{with: } \mathbf{z} = \Delta\dot{\mathbf{x}}_1 \tag{16}$$

Finally, based on the system identification results, regressive lead-lag is just an additional input denoted with **z**. This state equation is well-known in control theory as it is a common ansatz modelling disturbances. After Laplace-transformation, the system equation (15) is:

$$\begin{aligned}\mathbf{Z}(s) &= \mathbf{G}_{\Delta}\mathbf{U}(s) \\ &= \left(\mathbf{A}_{12}\left(s\mathbf{I}-\mathbf{A}_{22}\right)^{-1}\mathbf{B}_2+\mathbf{\Lambda}\right)\mathbf{U}(s)\end{aligned} \tag{17}$$

The overall frequency representation of equation (16) is

$$\begin{aligned}\mathbf{Y}(s) =& \mathbf{G}_{\mathbf{x}_1}\mathbf{U}(s)+(\mathbf{C}_1(s\mathbf{I}-\mathbf{A}_{11})^{-1})\mathbf{G}_{\Delta}\mathbf{U}(s) \\ \text{with: } \mathbf{G}_{\mathbf{x}_1} =& \left((\mathbf{C}_1(s\mathbf{I}-\mathbf{A}_{11})^{-1})\mathbf{B}_1+\mathbf{D}_1\right)\mathbf{U}(s)\end{aligned} \tag{18}$$

With equation (17) the additional input for roll and pitch acceleration is:

$$\begin{aligned}\Delta\ddot{p} =& G_{11}\delta_x + G_{12}\delta_y \\ \Delta\ddot{q} =& G_{21}\delta_x + G_{22}\delta_y\end{aligned} \tag{19}$$

Taking the first integral of equation (19) and performing an average for all airspeeds, this finally gives:

(20)

$$\frac{\Delta\dot{p}}{\delta_x} = \frac{0.1s-0.4}{s^2+1.0s+136} \qquad \frac{\Delta\dot{p}}{\delta_y} = \frac{-0.3s+2.0}{s^2+1.0s+136}$$
$$\frac{\Delta\dot{q}}{\delta_x} = \frac{-0.01s-0.1}{s^2+1.0s+136} \qquad \frac{\Delta\dot{q}}{\delta_y} = \frac{0.01s+0.01}{s^2+1.2s+136}$$

This equivalent model is used as an additional input for the nonlinear momentum equations of motions. An exemplary comparison between flight (grey curve) and nonlinear simulation (red curve) data is shown in figure 10. Without the equivalent model equation (20), the system simulator has a highly damped oscillation (red curve). The feedback gain is $K_p = 40$. This model helps develop appropriate resonance suppression algorithms but is only a simple equivalent model that do not replace nonlinear helicopter models.

6. Air Resonance Suppression

A former publication in this field [12] comes up with a controller that suppresses the oscillation well. The so called cross feed is a third order system that uses roll rate and its acceleration [12] to suppress air resonance. This approach (also referred to as p-ARS) has proven its performance and great robustness for rate and attitude feedback in several years of operation and for several configurations of the EC135 ACT/FHS. In future tasks, model-based control should be enhanced to arrive at in-flight simulation and rotor-state feedback assessment. This, however, requires high performances and feedback of angular acceleration or

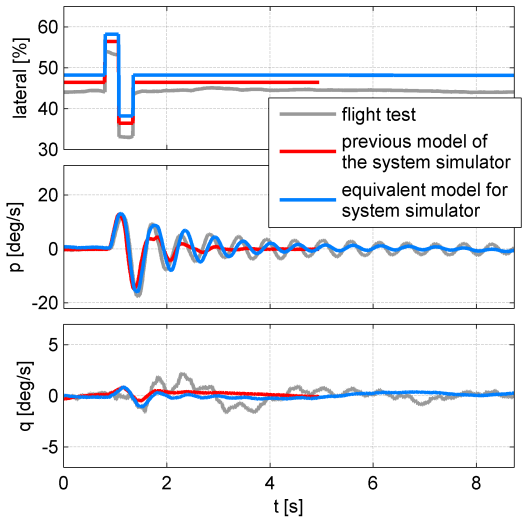

Figure 10: Comparison of roll and pitch rate response due to lateral cyclic control at 60 knot forward flight for ACT/FHS and nonlinear simulation (without-red and with-blue equivalent model), feedback gain $K_p = 40$

the lateral and longitudinal deflection of the main rotor's tip-path plane. The current air resonance controller needs approximately three oscillation cycles if the feedback gain is $K_p = 60$. If the feedback gain is further increased, the oscillation is more articulated and decreases performance. To further improve the performance especially for frequencies at $f \approx 10\,\mathrm{rad/s}$, air resonance suppression (denoted with ARS) should be improved. One opportunity is to readjust the cross feed. Another promising opportunity is to suppress air resonance by treating this phenomenon as a disturbance, equation (16), which is modelled as an additional control input. As the linear models derived by system identification allow the interpretation as a disturbance, the design of air resonance suppression is straight forward. The respective adapted suppression cancels this additional control signal and is called δ-ARS. For a first evaluation, however, the air resonance will be suppressed with simple systems. An overview is depicted in figure 11.

The dynamic system for δ-ARS is calculated as follows. Considering equation (16), lead-lag is just a disturbance and the equation is formulated as:

$$\begin{aligned}\dot{\mathbf{x}}_1 &= \mathbf{A}_{11}\mathbf{x}_1 + \mathbf{B}_1\left(\mathbf{u}+\mathbf{B}_1^{+}\mathbf{z}\right) \\ &= \mathbf{A}_{11}\mathbf{x}_1 + \mathbf{B}_1\mathbf{u}_z\end{aligned} \tag{21}$$

$\mathbf{B}_1^{+}$ is the pseudo-inverse of $\mathbf{B}_1$ and $\mathbf{B}_1^{+}\mathbf{z}$ transformed into the frequency domain is $\mathbf{Z}(s) = \mathbf{B}_1^{+}\mathbf{G}_{\Delta}\mathbf{U}(s)$ according to equation (17). From a modelling perspective, the controls $\mathbf{u}_z$ are calculated with

$$\mathbf{U}_z(s) = (\mathbf{I}+\mathbf{G}_{\Delta})\,\mathbf{U}(s) \tag{22}$$

and a possible compensation of air resonance is the inverse which is

$$\mathbf{U}(s) = (\mathbf{I}+\mathbf{G}_{\Delta})^{-1}\,\mathbf{U}_z(s) \tag{23}$$

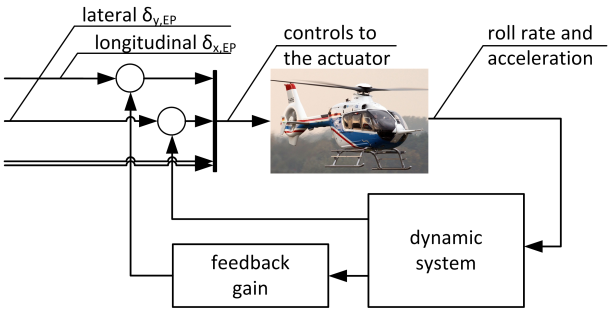

(a) Air resonance suppression (p-ARS) with a filtered roll rate [11, 12]

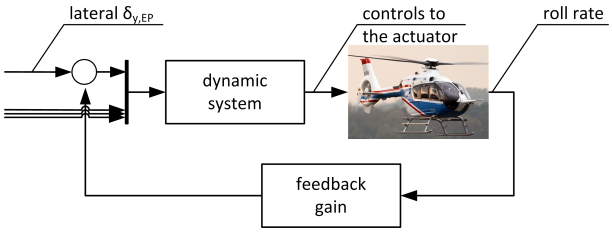

(b) Air resonance suppression (δ-ARS) with a filtered lateral control

Figure 11: Architectures for air resonance compensation

The inverse relies on pole-zero cancellation at least as exact as possible due to the pseudo-inverse $\mathbf{B}_1^+$. For simulation, this gives satisfactory results as lead-lag dynamics are nearly completely cancelled. The drawback is, that exact model knowledge is needed which is hardly to achieve for real aircraft but is still possible for nonlinear helicopter simulation such as SimH [20, 21] or linear models derived by system identification.

The inverse and dynamic system for air resonance suppression is then a coupled dynamic system with four inputs as well as outputs. The simulation result is shown in figure 12. If air resonance is compensated exactly (at least as best as possible with the pseudo-inverse approach equation (22)), the red curve in this figure is obtained. From simulation studies (see equation (20)) it could be observed, that the on-axis representation of the lateral control is sufficient to give satisfactory results concerning air resonance suppression (δ_y-ARS, blue curve). However, if the performance is still a matter, the respective dynamic system can easily enhanced with cross coupling terms. The structure of the on-axis inverse dynamic system is

$$\Delta_y(s) = K_y \left(1 + \frac{b_2 s^2 + b_1 s}{s^2 + 2D\omega_0 s + \omega_0^2 s^2}\right) \Delta_{y,z}(s) \tag{24}$$

$\Delta_y(s)$ denotes the lateral control of the actuator and $\Delta_{y,z}(s)$ is the control signal from the feedback controller. If this on-axis representation is applied to the lateral control, the blue curve in figure 12 can be simulated. The parameters are

$$\begin{aligned} &K_y = 1, \omega_0 = 12.6\,^{\mathrm{rad}}/_{\mathrm{s}}, D = .6, \\ &b_1 = .25, b_2 = -10.0 \end{aligned} \tag{25}$$

The key idea for this suppression is to define a right half plane zero. The initial system response thus is contrary to the input signal. Although the simulation shows that the exact suppression performs better, the suppression should cover a possibly wide range of frequencies as the air resonance phenomenon varies depending on meteorological conditions for instance [11, 12]. This can also be empirically motivated with the simple example. Assuming that closed-loop identification comes up with equation (11), then the exact compensator for air resonance suppression is

$$\Delta_y(s) = 1.8 \left(1 + \frac{.27s^2 + .42s}{s^2 + 3.4s + 185s^2}\right) \Delta_{y,z}(s) \tag{26}$$

If this dynamic system is used to suppress air resonance and the helicopter's response is described with equation (7), the closed-loop response is oscillating. To obtain a more robust suppression, especially the zeros of the dynamic system are strongly readjusted.

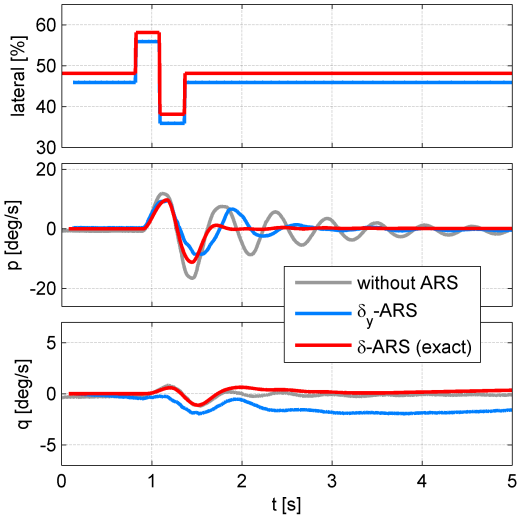

Figure 12: Roll and pitch rate response due to lateral control at 60 knot forward flight for the helicopter simulation, feedback gain $K_p = 40$

From simulation studies, the best way to adjust equation (24) is to use the initial values taken from partially closed-loop system identification. Then the following steps with moderate feedback gain (for the EC135 ACT/FHS $K_p = 40$) are hypothesized:

1. Adjust damping ratio D, obtain a oscillation with decreasing amplitude
2. Adjust eigenfrequency ω_0, obtain a faster suppression
3. Adjust b_1, reduce oscillation cycles
4. Adjust b_2, obtain a faster suppression

This approach is used for flight test and has proven its application. Air resonance suppression was adjusted in flight and ten settings were sufficient to decide for a feasible setting.

7. Flight Test Results With the EC135 ACT/FHS

The two suppression techniques (figure 11) together with pure roll rate feedback were flight-tested. The respective results are depicted in figure 13 and are discussed in the following.

The experimental pilot excited the oscillation with a computer-generated alternating step input and was then flying hands-off. As air resonance may yield an unstable response, the safety pilot took over control if the resonance could not be recovered by the controller.

Due to tight project deadlines and little availability of flight time, the configuration of the EC135 ACT/FHS varies. P-ARS and pure roll rate feedback were flight-tested with sensors installed [13] and δ_y-ARS was flight-tested with external hoist installed. This, however, may have an influence on the low-frequency dynamics as masses and inertia of the ACT/FHS vary but is not analysed explicitly. The meteorological conditions were similar except that the second flight test for δ_y-ARS was characterised by foehn and temperature was approximately twenty degree higher. Thus, air resonance was sometimes excited externally. However, results of both techniques are presented and compared although flight conditions are not exactly the same.

In figure 13 (a) time histories for 60 knot forward flight are depicted. Although both techniques use simple dynamic systems, the oscillation could be reduced. The pure roll rate feedback with $K_p = 60$ yield an unstable response and was recovered by the safety pilot after six seconds (not depicted). Both suppression techniques perform well. δ_y-ARS (adjusted similar to the simulation results except $b_2 = -50$) reduces the oscillation much faster (i.e. at $t = 3\,\mathrm{s}$) compared to p-ARS which needs one more second. Amplitudes of δ_y-ARS are generally smaller which may be caused by the different configuration and temperature. Pitch rate show nearly no oscillation for both techniques.

The computed frequency response data for roll and pitch rate for 60 knot forward flight are also shown in figure 13 (b) and (c). The phase for both techniques for the closed-loop is similar. The pitch and roll oscillation of the pure roll rate feedback is highly damped. The amplitudes of the oscillation (at approx. 11.5 rad/s) are minimised without increasing phase delay. The respective time-domain result in figure 13 (a) and the theoretical simulation study (figure 12) show that phase delay is not increased. δ_y-ARS performs slightly better for frequencies at approximately 10 rad/s.

The flight test results are promising especially as the adjustment of the δ_y-ARS can be achieved with less settings. Another advantage is that the structure of the respective dynamic system for suppression can be kept simple. Phase delay is not increased and the air resonance suppression should therefore improve handling qualities. This, however, is not part of this paper and will be analysed in future flight tests.

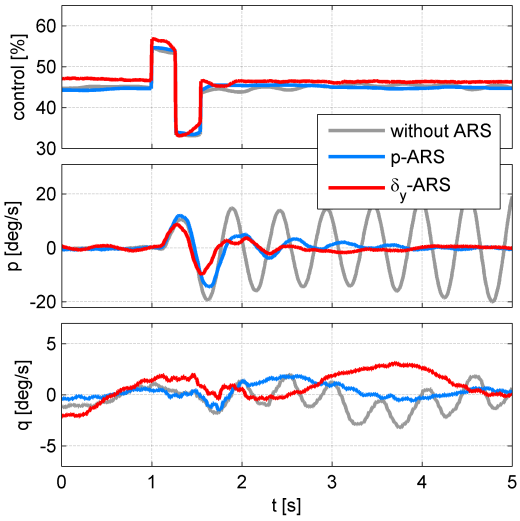

(a) Air resonance suppression (ARS), roll and pitch rate response

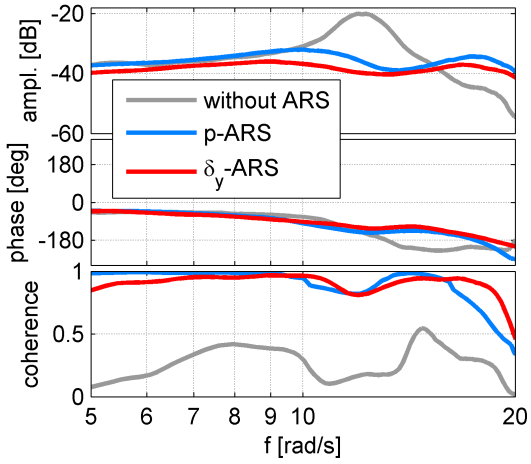

(b) Frequency response, roll rate

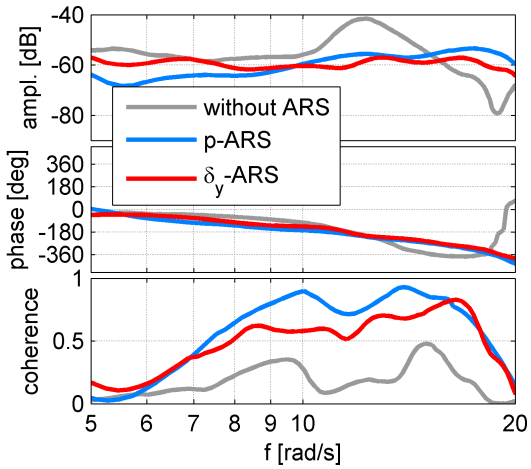

(c) Frequency response, pitch rate

Figure 13: Air resonance suppression (ARS) for 60 knot forward flight, feedback gain $K_p = 60$

8. Conclusion

Regressive lead-lag is a resonance phenomenon that occurs mainly for soft in-plane main rotors. The EC135 ACT/FHS shows this resonance if roll rate feedback with high gains is used. If the roll rate is filtered, the resonance can be suppressed and this method was used for six years and showed adequate performance and great robustness. Even a changed configuration of the ACT/FHS did only marginally affect the performance of the air resonance suppression but did affect the model parameters of the regressive lead-lag.

Due to new requirements for the closed-loop controller, air resonance suppression was analysed again. The goal was to suppress air resonance with an additional control input and regressive lead-lag is treated (from a modelling perspective) as a disturbance. The approach presented in this paper was kept similar to the one that was flight-tested over the past years. Again, only a simple dynamic system was used. The advantages are fast adjustment in flight and, again, good performance although only a simple on-axis system for the lateral control was used.

Future flight tests will cover more complex design methods to obtain better performance. As the theoretical limit from simulation studies shows, it is possible to arrive at nearly perfect suppression if the dynamic model of the regressive lead-lag is known exactly. This motivates the usage of adaptive control or at least disturbance estimation and feedforward.

Acknowledgement

This work is made possible through the support and assistance from Dr. Joachim Götz (DLR, Institute of Flight Systems). We would like to thank him for his encouragement and implementation of the lead-lag equations to the system simulator.

References

[1] R. E. Donham, S. V. Cardinale, and I. B. Sachs, "Ground and Air Resonance Characteristics of Soft In-Plane Rigidrotor System," *Journal of The American Helicopter Society*, vol. 14, no. 4, pp. 33–41, 1969.

[2] M. D. Pavel and G. D. Padfield, "Understanding the Peculiarities of Rotorcraft – Pilot – Couplings," in *AHS International 64th Annual Forum, Montreal, Canada*, April 29 - May 1, 2008.

[3] W. H. Weller, "Fuselage State Feedback for Aeromechanical Stability Augmentation of a Bearingless Main Rotor," *Journal of The American Helicopter Society*, vol. 41, no. 2, 1996.

[4] P. Almaras, "Active Control of Aeromechanical Stability Applied by Eurocopter," in *23rd European Rotorcraft Forum, Dresden, Germany*, September 16-18, 1997.

[5] F. K. Straub and W. Warmbrodt, "The Use of Active Controls to Augment Rotor/Fuselage Stability," *Journal of The American Helicopter Society*, vol. 30, no. 3, pp. 13–22, 1985.

[6] J. B. Dryfoos, B. D. Kothmann, and J. Mayo, "An Approach to Reducing Rotor-Body Coupled Roll Oscillations on the RAH-66 Comanche Using Modified Roll Rate Feedback," in *AHS International 58th Annual Forum, Montreal, Canada*, May 25-27, 1999.

[7] D. Teves, V. Klöppel, and P. Richter, "Development of Active Control Technology in the Rotating System, Flight Testing and Theoretical Investigations," in *18th European Rotorcraft Forum, Avignon, France*, September 15-18, 1992.

[8] G. Reichert and U. Arnold, "Active control of helicopter ground and air resonance," in *16th European Rotorcraft Forum, Glasgow, Scotland*, September 18-20, 1990.

[9] B. Panda, E. Mychalowycz, B. Kothmann, and R. Blackwell, "Active Controller for Comanche Air Resonance Stability Augmentation," in *AHS International 60th Annual Forum, Baltimore, Maryland*, June 07-10, 2004.

[10] V. Sahasrabudhe and P. J. Gold, "Reducing Rotor-Body Coupling Using active Control," in *AHS International 60th Annual Forum, Baltimore, Maryland*, June 07-10, 2004.

[11] M. Hamers, R. Lantzsch, and J. Wolfram, "First Control Evaluation of Research Helicopter FHS," in *33rd European Rotorcraft Forum, Kazaan, Russia*, September 11-13, 2007.

[12] R. Lantzsch, J. Wolfram, and M. Hamers, “Increasing Handling Qualities and Flight Control Performance using an Air Resonance Controller,” in *AHS International 67th Annual Forum, Montréal, Canada*, April 29 - May 1, 2008.

[13] R. Lantzsch, S. Greiser, J. Wolfram, J. Wartmann, M. Müllhäuser, T. Lüken, H. U. Döhler, and N. Peinecke, “ALLFlight: A Full Scale Pilot Assistance Test Environment,” in *AHS International 68th Annual Forum, Ft. Worth, TX*, May 01-03, 2012.

[14] J. Kaletka, H. Kurscheid, and U. Butter, “FHS, the New Research Helicopter: Ready for Service,” *Aerospace Science and Technology*, vol. 9, no. 5, pp. 456–467, 2005.

[15] S. Seher-Weiss and W. von Gruenhagen, “EC135 System Identification for Model Following Control and Turbulence Modeling,” in *Proceedings of the 1st CEAS European Air and Space Conference, Berlin*, pp. 2439–2447, 2007.

[16] M. Marchand and K. H. Fu, “Frequency Domain Parameter Estimation of Aeronautical Systems with and without Time Delay,” in *Proceedings of the 7th IFAC Symposium on Identification and System Parameter Estimation, York, UK*, pp. 669–674, July 3-7, 1985.

[17] M. B. Tischler and R. K. Remple, *Aircraft and Rotorcraft System Identification: Engineering Methods with Flight Test Examples*. Reston, VA: American Institute of Aeronautics and Astronautics, 2006.

[18] S. Greiser and S. Seher-Weiss, “A Contribution to the Development of a Full Flight Envelope Quasi-Nonlinear Helicopter Simulation,” in *Deutscher Luft- und Raumfahrtkongress, Berlin*, 10-12 September 2012.

[19] S. Greiser and W. von Gruenhagen, “Analysis of Model Uncertainties Using Inverse Simulation,” in *AHS International 69th Annual Forum, Phoenix, AZ*, May 21-23, 2013.

[20] M. Hamers and W. von Gruenhagen, “Nonlinear Helicopter Model Validation Applied to Realtime Simulations,” *Forum of the American Helicopter Society*, 1997.

[21] M. Hamers and W. von Gruenhagen, “Dynamic Engine Model Integrated in Helicopter Simulation,” *Forum of the American Helicopter Society*, 1998.